Modulation-mediated unlocking of a parametrically phase-locked spin torque oscillator

P. Dürrenfeld,[1] E. Iacocca,[1] J. Åkerman,[1,2] and P. K. Muduli[1,3]

[1)] *Department of Physics, University of Gothenburg, 412 96 Gothenburg, Sweden*

[2)] *Materials Physics, School of ICT, KTH-Royal Institute of Technology, Electrum 229, 164 40 Kista, Sweden*

[3)] *Department of Physics, Indian Institute of Technology, Delhi, 110016 New Delhi, India*

The ability of an oscillator to modulate is inevitable for its application in communication devices. While the output power and linewidth of single magnetic tunnel junction-based spin-torque oscillators (MTJ-STO) are not sufficient for practical uses, the synchronization of such devices can overcome these limitations. Here we investigate on the modulation behavior of a parametrically synchronized MTJ-STO and show experimentally that modulation of the synchronized state preserves synchronization as long as the modulation frequency, f_{mod}, is above a characteristic frequency, f_{unlock}. The unlocking frequency increases with the modulation amplitude in agreement with numerical simulations. These phenomena are analytically described as a non-resonant unlocking mechanism, whose characteristics are directly related to inherent parameters of the oscillator.

Magnetization precession at GHz frequencies can be sustained in spin-valve (SV) and magnetic tunnel-junction (MTJ) based spin-torque oscillators (STOs) as a result of spin transfer torque[1–4]. MTJ-STOs have attracted considerable interest because of their relatively large microwave power[5,6] and appreciable perpendicular spin torque [7–10]. However, these devices often exhibit a linewidth too large for practical applications. Injection locking offers means to decrease such large linewidths. Recently, both parametric excitation and synchronization have been achieved in MTJ-STOs[11–13], for which the external microwave current is applied at twice the frequency of the free-running MTJ-STO.

Synchronized MTJ-STOs exhibit a dramatic decrease of their linewidth, suggesting their preferable usage for wireless communication applications. In fact, injection-locked phase-locked loops (PLLs) are one of the most important building blocks of RF transceivers because they provide a precise frequency to transmit and receive data. It is hence essential to modulate the injection locked signals for both transmitters and receivers. Modulation of free-running STOs has been previously studied theoretically[14–16] as well as experimentally[17–19], demonstrating that these devices exhibit nonlinear frequency and amplitude modulation. The modulation of injection-locked STOs is yet to be addressed experimentally, complementing recent numerical studies[20].

The modulation of an injection-locked state faces the difficulty that the phase difference between the oscillator and the injection source is constant. This severely limits the possibility of modulating an injection-locked state. Here we show that it is possible to achieve fast modulation (up to 500 MHz) of the parametrically synchronized MTJ-STO. We show that the lower limit of modulation is determined by the modulation current and locking time of the MTJ-STO. These results are in qualitative agreement with macrospin simulations. By developing an analytical model, we quantitatively describe the observed modulation-mediated unlocking of the parametrically synchronized MTJ-STO. This has important consequences for both applications involving the synchronized STOs and for the fundamental understanding of the stability of a synchronized state.

The MTJ nanopillars used in this work are similar to those in Ref. 21. The layer structure consists of IrMn (5)/CoFe (2.1)/Ru (0.81)/CoFe (1)/CoFeB (1.5)/MgO (1)/CoFeB (3.5) (thicknesses in nm), where the bottom CoFe layer is the pinned layer (PL), the composite CoFe/CoFeB represents the reference layer (RL), and the top CoFeB layer is the free layer (FL). We discuss results from a *circular* device with an approximate diameter of 240 nm, a

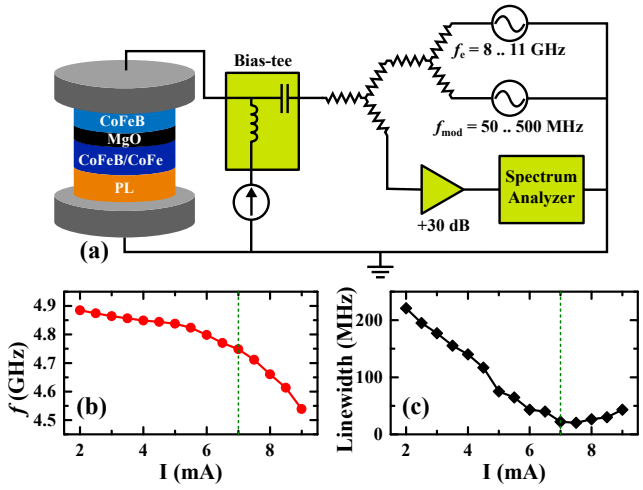

Figure 1. (color online). (a) The measurement circuit showing two signal sources connected with two power dividers for simultaneous modulation and parametric synchronization experiments. The oscillation frequency and linewidth of the free-running MTJ-STO are shown in (b) and (c), respectively. The parametric synchronization and modulation measurements are done at a bias current of $I_{DC} = 7$ mA, shown by the vertical dashed lines.

resistance-area product of 1.5 Ω μm^2, and a tunneling magnetoresistance of 75%. The RL magnetization equilibrium direction is along the positive $\hat{x}$-direction, which is also 0° of the applied field. Applying a positive current results in electrons flowing from the RL to the FL. An external magnetic field of 320 Oe is applied in-plane at an angle of 196° with respect to the RL magnetization to maximize the microwave power[22].

Our measurement circuit is shown in Fig. 1(a) where two signal sources are coupled into the AC port of the bias-tee through the use of two resistive power dividers (dc-12.5 GHz). The STO signal is fed to a +30 dB, 4-8 GHz low-noise amplifier (LNA) and then measured using a spectrum analyzer. The LNA operating frequencies were chosen to avoid amplification of both the injected signals. This allows us to apply rather strong external signals without saturating the LNA.

The free-running characteristics of our device, with both signal sources being turned off, are depicted in Fig. 1(b) and (c). Above $I_{DC} = 2$ mA, microwave signals can be detected in the spectrum analyzer with one clearly dominant mode at $f_0 \approx 4.8$ GHz. The STO frequency shows a slight red shift with increasing DC current. The transition from the thermally excited FMR-like oscillations to the auto-oscillation regime is found to be at $I_{th} = 6.2$ mA[23].

The linewidth of the free-running STO is shown in Fig. 1(c), which shows a typical decrease as a function of bias current and has a minimum at $I_{DC} \approx 7$ mA, which is slightly above the auto-oscillation threshold. For the experiments of parametric synchronization and modulation, we keep the driving current at a constant value of $I_{DC} = 7$ mA.

Figure 2 shows how the parametrically synchronized state of the MTJ-STO is established by injecting a microwave signal of approximately twice the frequency of the free-running STO from one of the signal generators. The microwave current from the signal source that reaches the device has a root-mean-square (rms) value of $I_e = 1.6$ mA, which is calculated by taking into account the losses due to the power dividers as well as the reflection coefficients measured by a vector network analyzer (VNA)[22]. Figure 2(a) shows the map of the power spectral densities (PSD) vs STO frequency and injected frequency. The injected frequency, f_{inj}, was swept between 9.0 GHz and 9.3 GHz in steps of 1 MHz while the spectrum analyzer's resolution bandwidth was kept at 50 kHz. This measurement shows that our device is successfully synchronized with a phase-locking bandwidth of approximately $f_{p-l} \approx 70$ MHz, which is an expected value for $I_e = 1.6$ mA_{rms}[13]. The linewidth of the MTJ-STO gets reduced to about 3 MHz from the free-running value of ≈45 MHz as shown in Fig. 2(b). While further reduction of the linewidth could be obtained using larger microwave currents I_e, we kept it fixed at 1.6 mA_{rms} to avoid sample breakdown during modulation.

To study the behavior of the parametrically synchronized MTJ-STO under modulation, the first signal source is fixed at the center of the locking bandwidth at a frequency of $f_e = 9.145$ GHz, while the frequency of the second signal source, f_{mod}, is varied in the range of 500 MHz $\geq f_{mod} \geq$ 50 MHz. Figure 3(a) shows an example of modulation of the parametrically synchronized MTJ-STO at $I_{mod} = 0.99$ mA, which clearly shows modulation sidebands at the frequencies $f + f_{mod}$, f - f_{mod}, and f - $2f_{mod}$. The asymmetric power of the sidebands is attributed to non-linear frequency and amplitude modulation (NFAM)[15,16,18]. This results in weaker power for the second order sideband at $f + 2f_{mod}$ and is expected from NFAM. However, the most important feature of this map is the breaking of synchronization for $f_{mod} \leq 170$ MHz, which we call the unlocking frequency: f_{unlock}. Above f_{unlock}, both the carrier and sidebands exhibit a narrow linewidth and the oscillation frequency of the carrier is exactly half of the injected frequency: $f = f_e/2$. However, for low modulation frequencies the carrier and sideband frequencies change to a lower value compared to the parametrically synchronized state. This is accompanied by an increase of linewidth to $\Delta f \approx 45$ MHz, which

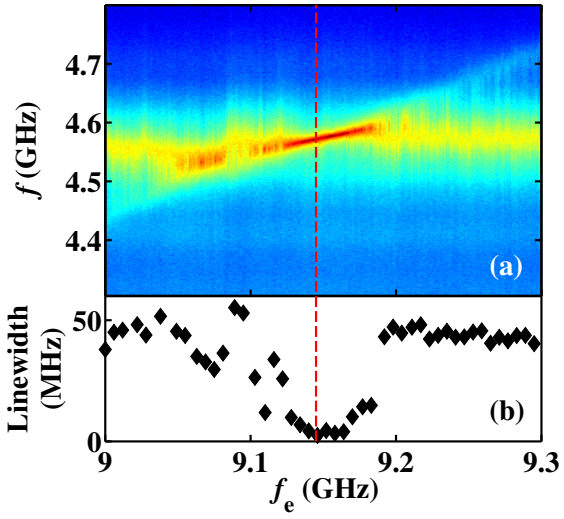

Figure 2. (color online). The parametric synchronization of the MTJ-STO, at I_{DC} = 7 mA, with an external signal of I_e = 1.6 mA, and $f_e \approx 2f_0$. (a) Spectrum and (b) linewidth of the STO vs. frequency of the external signal. The vertical dashed line marks the operating point for the modulation measurements.

corresponds to the free-running/unsynchronized linewidth at this condition [see Fig. 2(b)].

When the amplitude of the modulation signal is increased, f_{unlock} is shifted towards higher values. The observed variation between f_{unlock} and the modulation strength I_{mod}/I_{DC} is shown in Fig. 3(c) as black squares.

To further study this behavior we performed macrospin simulations. The magnetic parameters of the FL are taken from previous experimental studies on a similar device[21], namely: saturation magnetization $\mu_0 M_S$ = 1.25 T, Gilbert damping α = 0.01, symmetric spin torque efficiency η = 0.65, and field-like torque factor β = 0.5. All other parameters were taken from the experimental conditions. However, the threshold current obtained in macrospin simulations was found higher compared to experiment. In order to account for this difference, we use the diameter of the circular device as a free parameter and best agreement with experiment was obtained for a diameter of 140 nm. Figure 3(b) shows the simulated result obtained for the same external excitations as in the experiment. The figure shows clear unlocking for low f_{mod}, in good agreement with the experimental observations. Macrospin results of f_{unlock} as a function of the modulation strength I_{mod}/I_{DC} are shown in Fig. 3(c) as red circles. The f_{unlock} from numerical simulations shows a quantitative agreement with the experiments up until I_{mod}/I_{DC} = 0.2, above which the experiments deviate

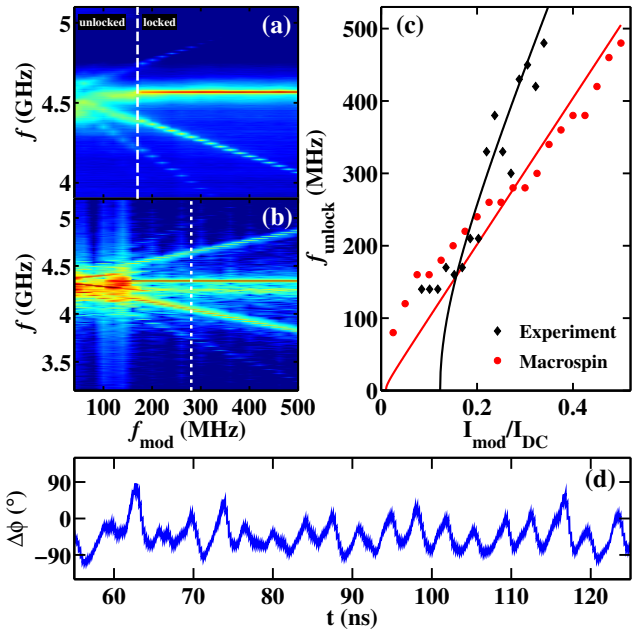

Figure 3. (color online). Modulation of a locked STO. (a) Experimental and (b) simulated spectra of the synchronized STO vs. f_{mod} at a modulation current of I_{mod} = 0.99 mA. (c) The relation between f_{unlock} and I_{mod}/I_{DC} shows a clear increase with I_{mod} for both experiments and numerical simulations. The solid lines are fits to the data according to eq. (1). (d) Section of the simulated instantaneous phase difference $\Delta\phi$ for the case of f_{mod} = 280 MHz, marked by a dashed line in (b).

from the numerical trend.

We will show below that the unlocking induced by the modulation can be well understood by a model considering the instantaneous phase and frequency differences between the MTJ-STO and the synchronizing signal, $f_e/2$, introduced by the modulating current. To develop such a model, the time scales involved in the experiment must be described in detail.

On one hand, the MTJ-STO is parametrically synchronized by an injection signal oscillating in the GHz range. However, the approach to synchronization occurs on a much larger time scale, on the order of 10 ns[24,25], which is equivalent to a frequency on the order of 100 MHz. Such a slow approach to synchronization is general in auto-oscillators[26]. On the other hand, the MTJ-STO is modulated by a signal oscillating in the MHz range. In the precessing reference of the free-running MTJ-STO, the modulating signal is slow enough so that it can be considered as a dc current, thus changing the free-running frequency of

the oscillator. That is precisely how the modulation in STO has been tackled analytically in previous studies[27]. The proposed model takes into account the slow approach to synchronization and the change of free-running conditions imposed by the modulation, both of which take place on the MHz range. In order to visualize these phenomena, we will describe the dynamics in terms of the instantaneous phase and frequency differences, $\Delta\phi$ and Δf, respectively. Both quantities are related by the proportionality $\Delta f \propto d\Delta\phi/dt$.

In line with the above experiments and simulations, we are considering a parametrically synchronized MTJ-STO. The synchronization condition indicates that there is a constant phase difference between the oscillator and the injection source, i.e. $\Delta\phi{=}\phi_o$ and $\Delta f{=}0$. When a slow modulating source is introduced, the free-running frequency of the MTJ-STO changes. Consequently, $\Delta\phi$ evolves in time until it reaches a new constant value $\Delta\phi{=}\phi_1 > \phi_o$ in order to stay synchronized. As the modulating source approaches its maximum amplitude, this process continues reaching a maximum phase difference $\Delta\phi{=}\phi_{max}$. Clearly, if $|\phi_{max}| > \pi$, the STO cannot lock anymore. Consequently, this description shows that there is a threshold modulating signal amplitude above which the MTJ-STO becomes unlocked.

Now, if the modulating frequency exceeds the approach to synchronization, f_{mod} >100 MHz, the above description breaks down. Instead, $\Delta\phi$ never achieves a stationary value and thus $\Delta f \neq 0$. The fact that the instantaneous frequency difference is non-stationary shows that it is possible to modulate a synchronized oscillator, as experimentally and numerically observed in Fig. 3(a) and (d), respectively. However, it also becomes unclear how to model the unlocking condition in this case. The solution is to acknowledge that the aforementioned unlocking condition, $|\phi_{max}| > \pi$, is equivalent to $|\Delta f_{max}| > f_{p-l}$ in the non-stationary case. In other words, the instantaneous frequency difference induced by the modulation source cannot surpass the phase locking bandwidth for a given injection current I_e. Consequently, we can model the unlocking behavior simply by taking into account the modulation characteristics of Δf for a free-running MTJ-STO. A previous analytical study on the modulation of STOs[27] showed that Δf_{max} is given by

$$\Delta f_{max} = 2\nu\Gamma_p\Gamma_-(p_o)\frac{\mathrm{I}_{mod}}{\mathrm{I}_{DC}}\frac{1}{\sqrt{4\Gamma_p^2 + f_{mod}^2}}, \tag{1}$$

where $\nu \approx 1$ is the dimensionless nonlinearity coefficient, Γ_p is the total damping rate, and $\Gamma_-(p_o)$ is the negative damping term at a given operating point. Imposing the unlocking

condition $\Delta f_{max} = f_{p-l}$ for $f_{mod} = f_{unlock}$, one can fit Eq. 1 as a function of $\Gamma_-(p_o)$. In agreement with the above qualitative understanding, Eq. 1 leads to a threshold modulating amplitude for a vanishingly slow modulation frequency, $f_{mod} \ll 2\Gamma_p$. Furthermore, Eq. 1 now relates the unlocking frequency to the experimental quantities f_{mod} and f_{p-l}. In particular, as f_{p-l} increases, the STO will be able to sustain a stronger modulation current and slower modulation frequencies. This conclusion is in agreement with the numerical results presented in a recent study[20] where the above unlocking was identified as a *non-resonant* mechanism.

The fits of the experimental and numerical results using Eq. 1 are shown in Fig. 3(c) by black and red solid lines, respectively. For both cases, we obtain $\Delta f_{max} \approx 0.1\Gamma_-(p_o)$ which is consistent with the fact that the modulation is a perturbation on the stable oscillation. Furthermore, the fits give insight into the intrinsic negative damping term which can be fitted to the analytical theory by polynomial expansions[11,28]. The difference between the two fits originates from the values of Γ_p. In fact, previous measurements on a similar MTJ-STO device[23] showed that $\Gamma_p \approx 100$ MHz, which is much higher than the theoretically expected $\sim$5 MHz [calculated using Eq. (27b) in Ref. 14]. Such an inconsistency is related to the multi-mode generation proper of these devices that has been addressed theoretically only recently[27,29]. In the case of macrospin simulations, multi-mode generation cannot be modeled as they originate from the micromagnetic details of the device's active layer. Consequently, we are able to fit the results by using the theoretical Γ_p. A better agreement with experiments is expected from a micromagnetic model of the device. This is, however, beyond the scope of the present letter.

As mentioned before, the macrospin simulation quantitatively agrees with the experimental data for $I_{mod}/I_{DC} < 0.2$. From the above analysis and fits we argue that such agreement can entail that the weakly perturbed MTJ-STO behaves in a nearly single mode regime, thus having an effective Γ_p closer to the analytical estimate and making the macrospin simulation more accurate. Furthermore, the disagreement with the analytical estimates suggests that nonlinear processes are taking place when $f_{unlock} \approx 150$ MHz. It is possible that such a regime is characterized by a competition between the modulation-mediated unlocking and the ability of the device to synchronize, limited by the synchronization time of $1/150$ MHz ~ 6.7 ns, in agreement with recent experiments[25].

In summary, we have presented experimental and numerical proofs of modulation-mediated unlocking in MTJ-STOs. It is argued that such a phenomenon is possible due

to the non-resonant unlocking mechanism. These results are relevant for the design of synchronized STO-based devices for communication applications where modulation is an instrumental phenomenon. Moreover, the presented experimental method can be used and extended to determine STO figures-of-merit such as the modulation index and the modulation bandwidth.

J.Å. and P.K.M. gratefully acknowledge support from the Swedish Research Council (VR). J.Å. was also supported from the Swedish Foundation for Strategic Research (SSF) and is a Royal Swedish Academy of Sciences Research Fellow supported by a Grant from the Knut and Alice Wallenberg Foundation.

REFERENCES

[1]J. C. Slonczewski, J. Magn. Magn. Mater. **159**, L1 (1996).

[2]L. Berger, Phys. Rev. B **54**, 9353 (1996).

[3]M. Tsoi, A. G. M. Jansen, J. Bass, W.-C. Chiang, V. Tsoi, and P. Wyder, Nature **406**, 46 (2000).

[4]S. I. Kiselev, J. C. Sankey, I. N. Krivorotov, N. C. Emley, R. J. Schoelkopf, R. A. Buhrman, and D. C. Ralph, Nature **425**, 380 (2003).

[5]A. M. Deac, A. Fukushima, H. Kubota, H. Maehara, Y. Suzuki, S. Yuasa, Y. Nagamine, K. Tsunekawa, D. D. Djayaprawira, and N. Watanabe, Nat. Phys. **4**, 803 (2008).

[6]A. V. Nazarov, H. M. Olson, H. Cho, K. Nikolaev, Z. Gao, S. Stokes, and B. B. Pant, Appl. Phys. Lett. **88**, 162504 (2006).

[7]A. A. Tulapurkar, Y. Suzuki, A. Fukushima, H. Kubota, H. Maehara, K. Tsunekawa, D. D. Djayaprawira, N. Watanabe, and S. Yuasa, Nature **438**, 339 (2005).

[8]J. C. Sankey, Y.-T. Cui, J. Z. Sun, J. C. Slonczewski, R. A. Buhrman, and D. C. Ralph, Nat. Phys. **4**, 67 (2008).

[9]O. G. Heinonen, Phys. Rev. B **81**, 054405 (2010).

[10]S. Oh, S. Park, A. Manchon, M. Chshiev, J. Han, H. Lee, J. Lee, K. Nam, Y. Jo, Y. Kong, B. Dieny, and K. Lee, Nat. Phys. **5**, 898 (2009).

[11]S. Urazhdin, V. Tiberkevich, and A. Slavin, Phys. Rev. Lett. **105**, 237204 (2010).

[12]M. Quinsat, D. Gusakova, J. F. Sierra, J. P. Michel, D. Houssameddine, B. Delaet, M.-C. Cyrille, U. Ebels, B. Dieny, L. D. Buda-Prejbeanu, J. A. Katine, D. Mauri, A. Zeltser,

M. Prigent, J.-C. Nallatamby, and R. Sommet, Appl. Phys. Lett. **97**, 182507 (2010).

[13]P. Dürrenfeld, E. Iacocca, J. Åkerman, and P. K. Muduli, Appl. Phys. Lett. **104**, 052410 (2014).

[14]A. Slavin and V. Tiberkevich, IEEE Trans. Magn. **45**, 1875 (2009).

[15]G. Consolo, V. Puliafito, L. Lopez-Diaz, F. Nizzoli, L. Giovannini, G. Valenti, and B. Azzerboni, IEEE Trans. Magn. **46**, 3629 (2010).

[16]E. Iacocca and J. Åkerman, Phys. Rev. B **85**, 184420 (2012).

[17]M. R. Pufall, W. H. Rippard, S. Kaka, T. J. Silva, and S. E. Russek, Appl. Phys. Lett. **86**, 082506 (2005).

[18]P. K. Muduli, Y. Pogoryelov, S. Bonetti, G. Consolo, F. Mancoff, and J. Åkerman, Phys. Rev. B **81**, 140408 (2010).

[19]Y. Pogoryelov, P. K. Muduli, S. Bonetti, E. Iacocca, F. Mancoff, and J. Åkerman, Appl. Phys. Lett. **98**, 192501 (2011).

[20]E. Iacocca and J. Åkerman, Phys. Rev. B **87**, 214428 (2013).

[21]P. K. Muduli, O. G. Heinonen, and J. Åkerman, Phys. Rev. B **83**, 184410 (2011).

[22]P. K. Muduli, O. G. Heinonen, and J. Åkerman, J. Appl. Phys. **110**, 076102 (2011).

[23]P. K. Muduli, O. G. Heinonen, and J. Åkerman, Phys. Rev. Lett. **108**, 207203 (2012).

[24]Y. Zhou, V. Tiberkevich, G. Consolo, E. Iacocca, B. Azzerboni, A. Slavin, and J. Åkerman, Phys. Rev. B **82**, 012408 (2010).

[25]W. Rippard, M. Pufall, and A. Kos, Appl. Phys. Lett. **103**, 182403 (2013).

[26]A. Pikovsky, M. Rosenblum, and J. Kurths, *Synchronization: A universal concept in nonlinear sciences* (Cambridge University Press, 2001).

[27]E. Iacocca, O. Heinonen, P. K. Muduli, and J. Åkerman, Phys. Rev. B **89**, 054402 (2014).

[28]Ezio Iacocca and Johan Åkerman, J. Appl. Phys. **110**, 103910 (2011).

[29]O. Heinonen, Y. Zhou, and D. Li, arXiv:1310.6791 [cond-mat.mes-hall] (2013).